Supplementary Information (SI) for Nanoscale.

Supporting Information

Effect of Grain Boundaries on Metal Atom Migration and Electronic Transport in 2D TMD-based Resistive Switches

Mohit D. Ganeriwala,*,† Daniel Luque-Jarava,† Francisco Pasadas,† Juan J. Palacios,‡ Francisco G. Ruiz,† Andres Godoy,*,† and Enrique G. Marin*,†

†*Department of Electronics and Computer Technology, University of Granada, 18071, Granada, Spain*

‡*Departamento de Física de la Materia Condensada, Universidad Autónoma de Madrid, 28049 Madrid, Spain*

E-mail: mohit@go.ugr.es; agodoy@ugr.es; egmarin@go.ugr.es

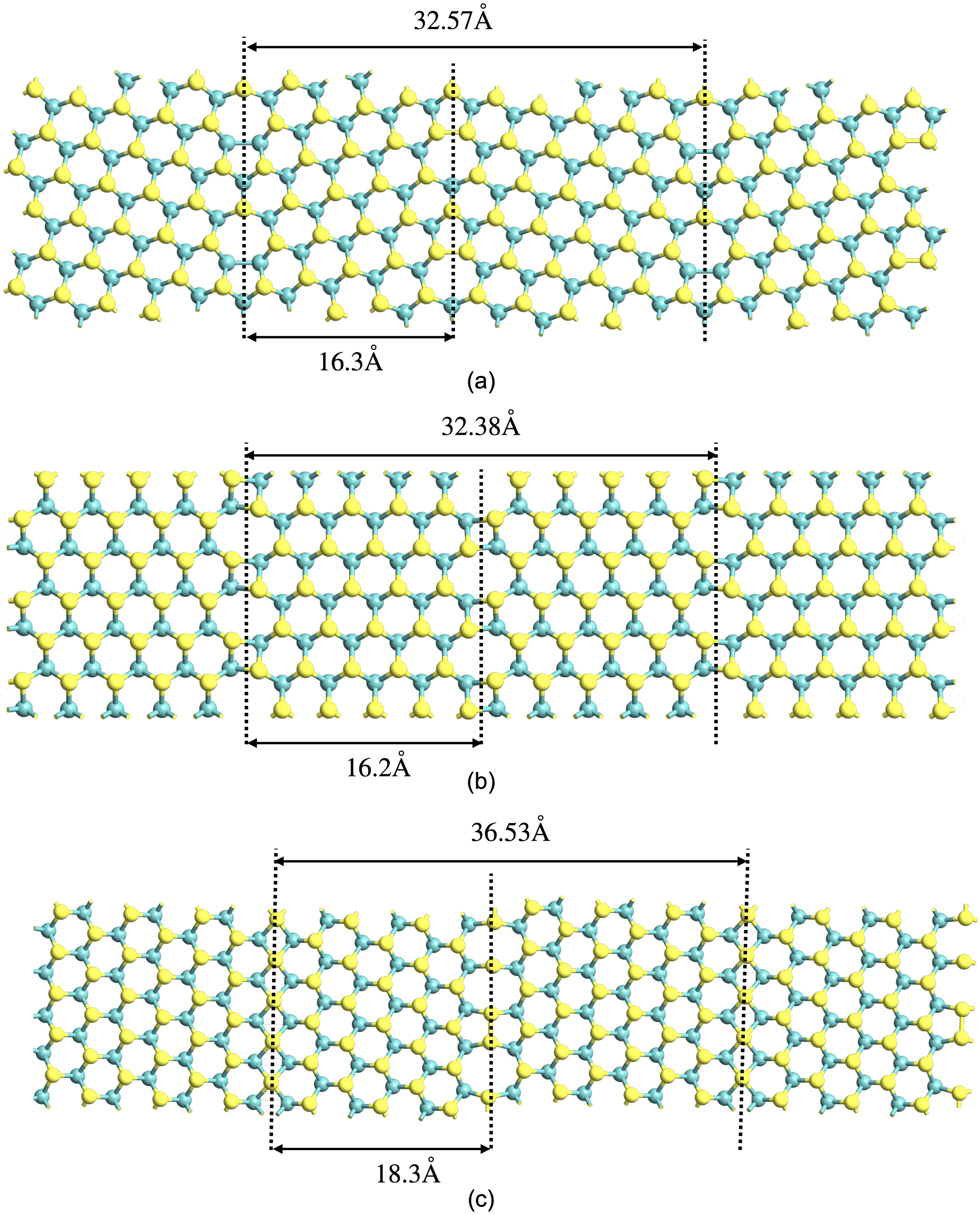

Figure S1: MoS_2 extended supercell for (a) 22° (b) 60° (ZZ) and (c) 60° (AC) grain boundary displaying the periodic boundary condition, as utilized in this study. Each supercell used in the simulation contains two anti-parallel grain boundary separated by at least 16 Å and the distance between the periodic image of the grain boundary is at least 32 Å.

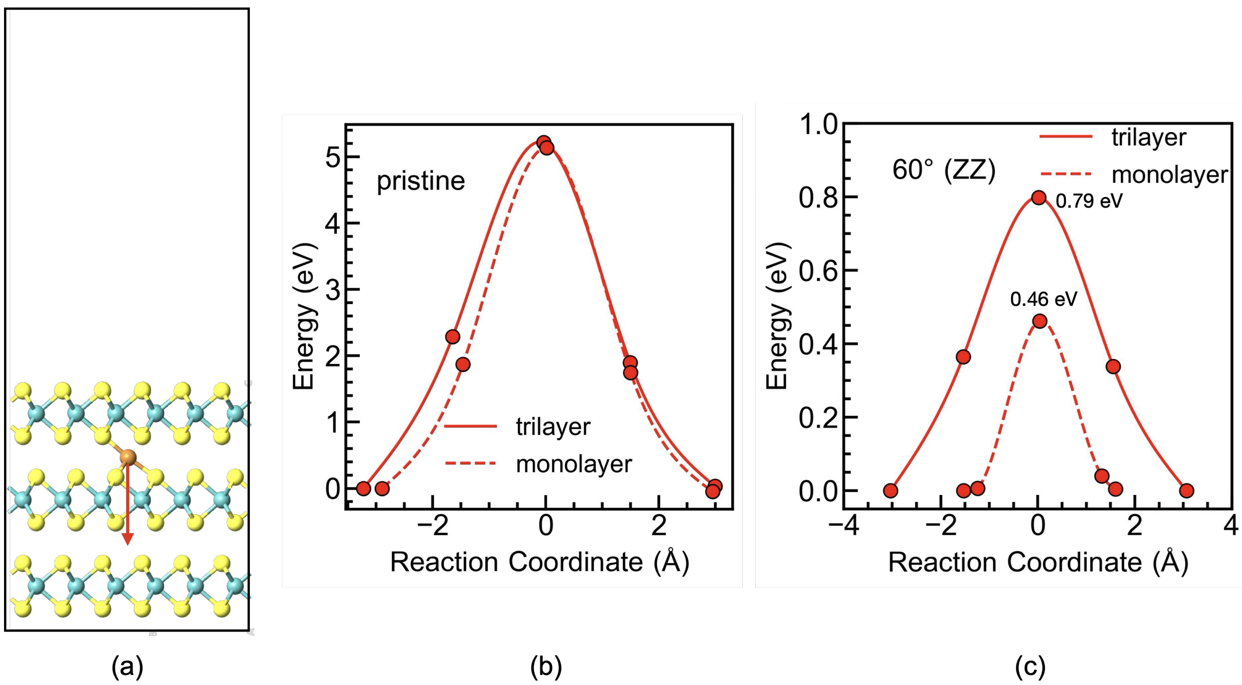

Figure S2: (a) Supercell of a trilayer MoS_2 showing the diffusion of a metallic atom across a layer. Comparison of the diffusion barrier for Copper across MoS_2 in the monolayer and trilayer cases for (b) pristine and (c) 60° (ZZ) grain boundary (GB). The presence of additional layers above and below the diffusion layer has a negligible impact on the barrier for pristine MoS_2. However, for the GB case, a change in the barrier is observed, although small (0.46 eV in monolayer to 0.79 eV in trilayer). This can be attributed to the attractive force exerted by the adjacent layers as it was already seen to cause a reduction in the distance between the MoS_2 and the metal atom, $d_{\text{Cu-Mo}}$ in presence of GBs (see Fig. 2c of the manuscript).

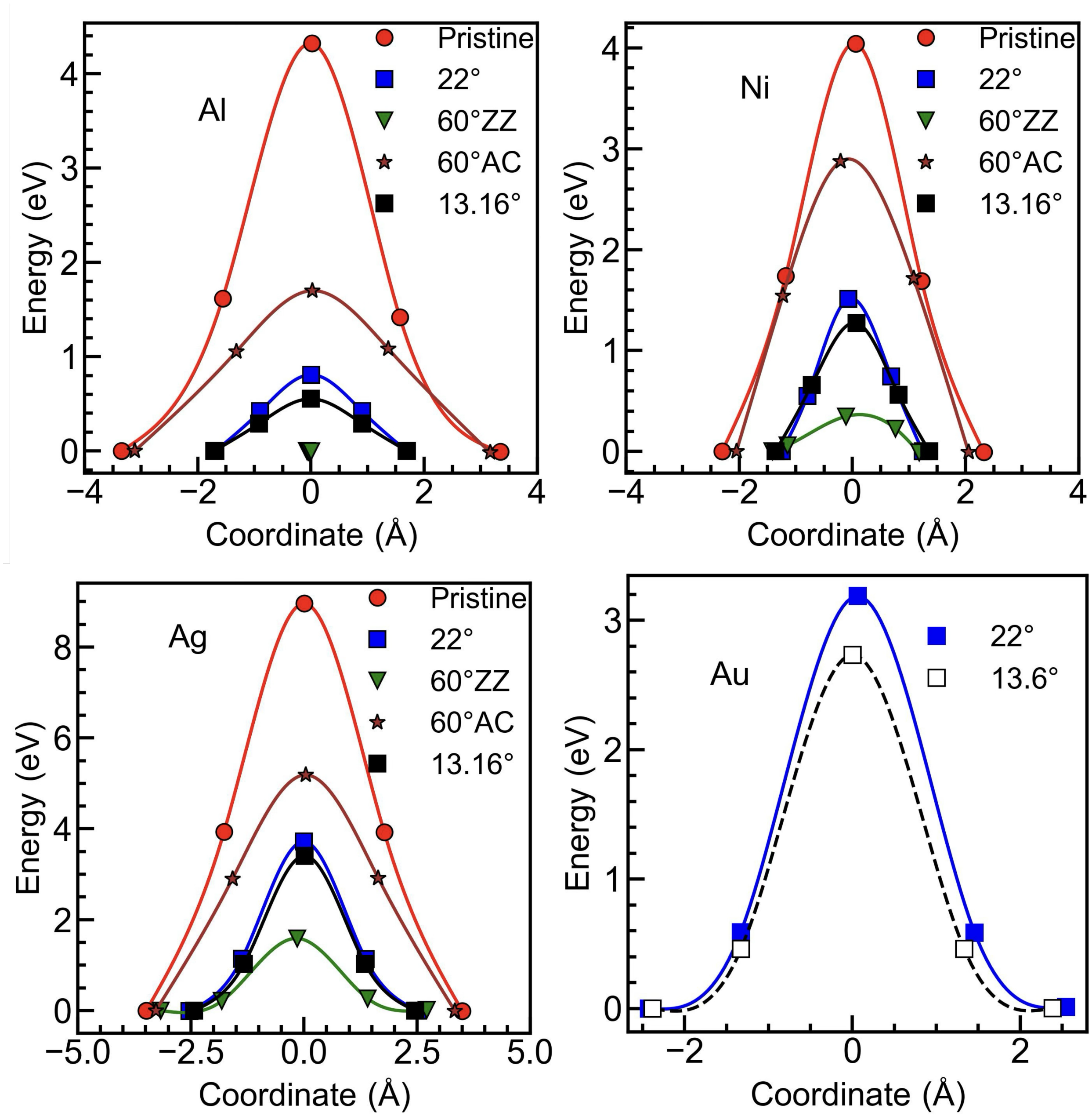

Figure S3: Barrier for out-of-plane diffusion plotted along the minimum energy path as a function of the distance traveled with respect to the MoS_2 plane. The barrier is calculated and plotted for Aluminium (Al), Nickel (Ni) and Silver (Ag) for pristine, and grain boundaries with tilt angle of 22° 60° ZZ, 60° AC and 13.16°. The diffusion barrier for Gold (Au) is plotted for a 13.16° grain boundary and compared with a 22° grain boundary, which also results in 5—7 dislocation cores with different distances among them. These barriers correspond to the values reported in Table 1 of the manuscript.

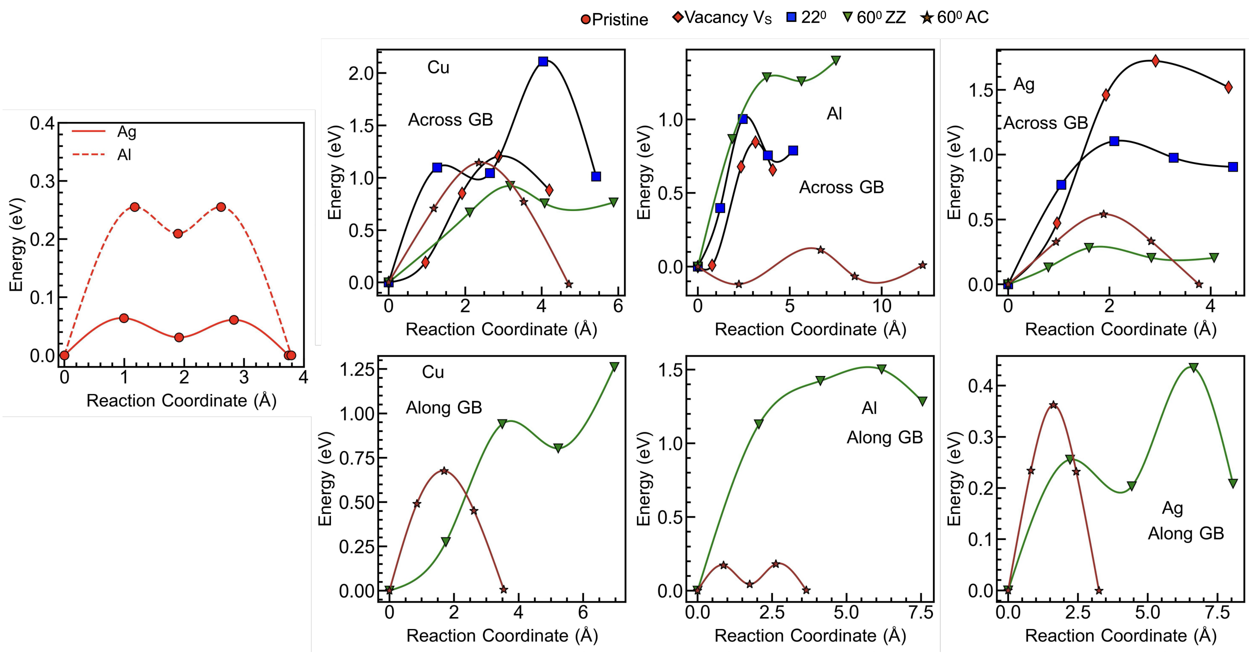

Figure S4: Barrier for the diffusion on the surface of MoS_2 plotted along the minimum energy path as a function of the reaction coordinate. The barrier is plotted first for Aluminium (Al) and Silver (Ag) for pristine MoS_2, and next for Copper (Cu), Al, and Ag for grain boundaries with tilt angle of 22°, 60° ZZ and 60° AC. The barriers are plotted for diffusion both across (top row) and along (bottom row) the grain boundaries. These barriers correspond to the values reported in the Table 2 of the manuscript.

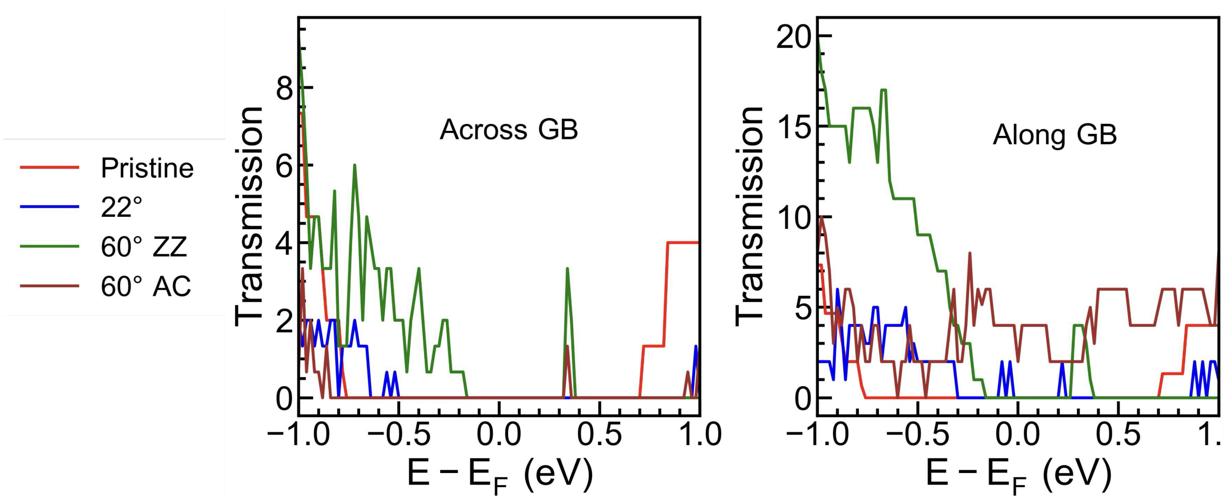

Figure S5: Transmission spectrum for transport both across and along the grain boundaries with tilt angle of 22°, 60° ZZ and 60° AC, as well as for in-plane transport for pristine MoS_2.

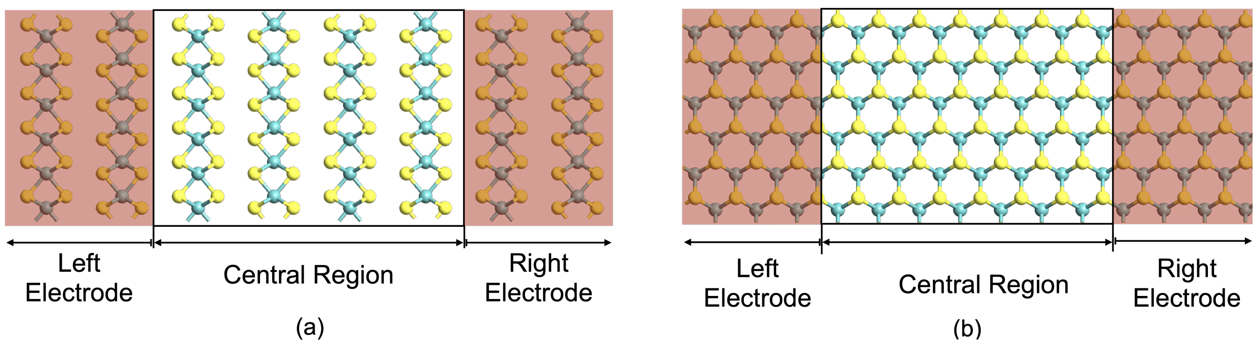

Figure S6: Device setup used for the calculation of electron transport in the (a) out-of-plane direction and (b) in-plane direction of a MoS_2. A bulk structure, periodic in the x, y, and z directions, is used for out-of-plane transport, while a monolayer periodic in the y and z directions, with z defining the direction of transport, is used for in-plane transport analysis. Here, MoS_2 acts as the left and right leads with the same configuration as the central region to avoid any interface effects.